Floppy Fluid Vesicles in Elongational Flow

G. Gompper[1] and D. M. Kroll[2]
[1]*Sektion Physik der Ludwig-Maximilians-Universität München, Theresienstrasse 37, 8000 München 2, Germany*
[2]*Institut für Festkörperforschung, Kernforschungsanlage Jülich, Postfach 1913, 5170 Jülich, Germany*
(Received 24 February 1993)

The behavior of self-avoiding fluid vesicles in elongational flow is studied using Monte Carlo simulations and scaling arguments. The simulations are carried out for membranes with a very small bending rigidity, in the free-draining approximation. We find that there is a gradual crossover from self-avoiding branched-polymer to elongated linear-polymer behavior as the flow rate is increased. At small flow rates, our results scale with the relaxation time of undisturbed branched polymers. The scaling behavior is the same in both unidirectional and planar flow geometries.

PACS numbers: 87.22.Bt, 05.40.+j, 36.20.-r

Membranes are two-dimensional sheets of molecules which form spontanously when amphiphiles or lipids are added to water [1,2]. They usually form closed surfaces called vesicles in order to prevent contact between the hydrocarbon chains of the lipid molecules and water. Since membranes are (nearly) tensionless surfaces, the shape of a vesicle is controlled by a delicate interplay between thermal fluctuations, the elastic bending energy [3], the osmotic pressure difference between the vesicle interior and exterior, the pH of the solvent, and possible constraints such as fixed volume or surface area. When the persistence length [4] of the membrane is large compared to the diameter of the vesicle—which is the case for most vesicles studied in experiment [5]—the vesicle shape minimizes the elastic energy, consistent with any constraints on the area and volume. On the other hand, when the persistence length is much smaller than the typical vesicle size, the shape of the vesicle is controlled by thermal fluctuations. Such floppy vesicles have indeed been observed experimentally [6].

There has been considerable progress recently in understanding the statistical thermodynamics and structure of these systems (for reviews, see Refs. [7,8]). Little, however, is known about their nonequilibrium behavior and rheology. In this paper we present the first analysis of the behavior of fluid vesicles embedded in an external flow field. In particular, we consider the case of elongational flow. This type of flow field occurs, for example, at the entry of a capillary. It represents a unidirectional external perturbation which breaks the rotational invariance of the bending Hamiltonian. It is one of the simplest flow geometries to analyze since the vesicle still has a *stationary* probability distribution. This work is intended as a first step towards understanding the behavior of vesicles, liposomes, and erythrocytes [9,10] in more general flow geometries.

The velocity field $\mathbf{v}$ of the solvent at position $\mathbf{r}$ can be written in the general form

$$\mathbf{v}(\mathbf{r}) = \Gamma(\mathbf{r})\mathbf{r}. \tag{1}$$

The simplest nontrivial case is elongational (or extensional) flow [11], where the flow is incompressible, $\nabla\cdot\mathbf{v} = 0$, and the flow tensor Γ is diagonal and independent of $\mathbf{r}$,

$$\Gamma = \begin{pmatrix} -s/2 & 0 & 0 \\ 0 & -s/2 & 0 \\ 0 & 0 & s \end{pmatrix}. \tag{2}$$

s is the flow rate. Such a flow field can be realized experimentally by a system of two opposed capillaries, where the solvent is pumped into (or sucked out of) both capillaries with the same flow rate [12]. When hydrodynamic interactions are neglected—which we will do throughout this paper—the flow of the solvent exerts a force $\mathbf{F}(\mathbf{r}) = \eta\mathbf{v}(\mathbf{r})$ on a piece of membrane located at $\mathbf{r}$. Our use of the free-draining approximation is motivated by the complexity of the system under consideration. Any more realistic model for vesicles has to take into account the condition that no solvent flow occurs perpendicular to the membrane. In the free-draining approximation, the motion of a point $\mathbf{R}$ on the vesicle surface is thus determined by the Langevin equation

$$\frac{\partial}{\partial t}\mathbf{R} = \mathbf{v}(\mathbf{R}) + \frac{\delta\mathcal{H}}{\delta\mathbf{R}} + \zeta\,, \tag{3}$$

where $\mathcal{H}[\mathbf{R}]$ is the curvature Hamiltonian together with self-avoidance constraints and ζ is a Gaussian white noise. Here, we have absorbed the viscosity η of the solvent into the flow rate s. For any flow with a symmetric, space-independent flow tensor Γ, the flow can be written as the derivative of a potential

$$V[\mathbf{r}] = \frac{1}{2}\mathbf{r}\Gamma\mathbf{r}\,, \tag{4}$$

so that $\mathbf{v}(\mathbf{r}) = \delta V/\delta\mathbf{r}$. Thus, we can define a new Hamiltonian,

$$\mathcal{H}_{\rm flow} = \mathcal{H} + V\,, \tag{5}$$

and study the equilibrium thermodynamics of a vesicle described by the Hamiltonian (5).

The behavior of dilute, flexible *polymers* in various

types of flow fields has been studied extensively in recent years [11]. In elongational flow, the radius of gyration R_g of a polymer consisting of N monomers shows the scaling behavior [11,13]

$$\langle R_g^2(s,N)\rangle = N^{2\nu_{\rm lin}}\Theta(sN^{1+2\nu_{\rm lin}}) \quad (6)$$

for small flow rates, where, in three dimensions, $\nu_{\rm lin} \simeq 3/5$ is the self-avoiding random walk exponent. The simplest way to understand this scaling form is to note that the flow rate s has the dimension of inverse time. Thus, the product $s\tau$ of the flow rate with the longest relaxation time τ is the appropriate scaling variable. The relaxation time τ is proportional to the time it takes for the polymer to diffuse over a distance equal to its radius of gyration [11], i.e.,

$$\tau \sim \langle R_g^2\rangle/D \sim N^{1+2\nu_{\rm lin}}, \quad (7)$$

where $D \sim 1/N$ is the mobility of the entire chain in Rouse dynamics. It has been suggested by de Gennes [14] that a first-order coil-stretch transition occurs in elongational flow, from an essentially undisturbed, coiled polymer chain with the scaling behavior (6) at low flow rates to a stretched, linear configuration at high flow rates. The stretch-coil transition should occur at $s \sim N^{-(1+2\nu_{\rm lin})}$. There is both experimental [15] and theoretical [16,17] evidence that a first-order stretch-coil transition does *not* occur. However, a crossover from coiled to stretched configurations, or a fracture of the chain [17], should take place at $s\tau \simeq 1$.

We have performed extensive Monte Carlo simulations for a simple tether-and-bead model of fluid vesicles in elongational flow. The model consists of N spherical beads of diameter $\sigma = 1$, which are connected by tethers of length $\ell = \sqrt{2}$ to form a two-dimensional, triangular network of spherical topology. A Monte Carlo step (MCS) consists of an attempt to move all beads sequentially by a random increment in the cube $[-\delta r, \delta r]^3$, followed by an attempt to flip N randomly selected tethers. Details of this simulation procedure can be found in Refs. [18–22]. We choose $\delta r = 0.1$ here, so that about 50% of the position updates are accepted. We have simulated vesicles with $N = 127$, 247, and 407 monomers. Averages are taken over runs of $(25\text{–}100)\times 10^6$ MCS (per monomer). To prevent the vesicle from leaving the center of the flow during the simulation, the center of flow is readjusted after each MCS to the center of mass of the vesicle.

To characterize the conformation of a vesicle in elongational flow, we study the eigenvalues $\lambda_1 \le \lambda_2 \le \lambda_3$ of the moment of inertia tensor,

$$\mathcal{T}_{\alpha,\beta} = \frac{1}{N}\sum_i (r_{i\alpha}r_{i\beta} - \bar r_\alpha \bar r_\beta), \quad (8)$$

where $\alpha, \beta \in \{x, y, z\}$, and the sum runs over all vertices of a given configuration; $\bar r_\alpha$ is the α component of the center of mass for that configuration. In particular, we calculate the radius of gyration,

$$\langle R_g^2\rangle = \sum_{i=1}^{3}\langle\lambda_i\rangle, \quad (9)$$

the asphericity [23]

$$\Delta_3 = \frac{\langle\lambda_1^2+\lambda_2^2+\lambda_3^2-(\lambda_1\lambda_2+\lambda_2\lambda_3+\lambda_3\lambda_1)\rangle}{\langle(\lambda_1+\lambda_2+\lambda_3)^2\rangle}, \quad (10)$$

and the fluctuations of the radius of gyration,

$$\chi_g = \sqrt{\langle(R_g^2)^2\rangle - \langle(R_g^2)\rangle^2}. \quad (11)$$

The asphericity Δ_3 vanishes for completely spherical conformations, while $\Delta_3 \to 1$ in the limit of very long cigar shapes; in general, $0 \le \Delta_3 \le 1$.

It has been shown previously [20–22,24] that the scaling behavior of fluid vesicles with small bending rigidities κ subject to sufficiently small or vanishing pressure increments Δp belongs to the branched-polymer universality class [25] which is characterized by a radius of gyration exponent [26] $\nu_{\rm bp} = 1$. When the elongational flow is turned on, the radius of gyration and the asphericity Δ_3 increase. Thus, the vesicle becomes elongated, as expected. Our results as a function of the scaled flow rate are shown in Figs. 1 and 2, for both uniaxial ($s > 0$) and planar ($s < 0$) flow. For small flow rates, the data are consistent with the scaling form [26,27]

$$\Delta_3 = \Psi(sN^\gamma),$$
$$\langle R_g^2\rangle = N^\nu\Theta(sN^\gamma), \quad (12)$$

with $\gamma = 2$ and $\nu = \nu_{\rm bp} = 1$. In order to take finite size corrections into account, N has been replaced by $N - N_0$ in the scaling argument of Eq. (12); a similar shift in the N dependence of $\langle R_g^2\rangle$ at $s = 0$ has also been performed [22,28]. At flow rates $s(N-N_0)^\gamma \simeq 25$–75, a strong increase in Δ_3 is observed, which signals a crossover from a spherical to a cigar shape. Note that during this initial elongation the radius of gyration only increases by about a factor of 2. Only at larger flow rates does the radius of gyration begin to increase more strongly. In this region, the vesicle has only a very small number of short branches, and it is reasonable to assume

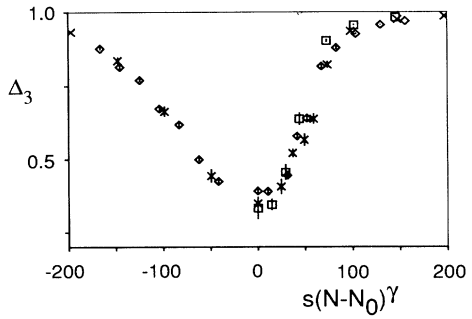

FIG. 1. Aspericity Δ_3 as a function of the scaled flow rate $s(N-N_0)^\gamma$, with $\gamma = 2$ and $N_0 = 25$. Data are shown for $N = 127$ ($\diamond$), $N = 247$ ($\times$), and $N = 407$ ($\square$).

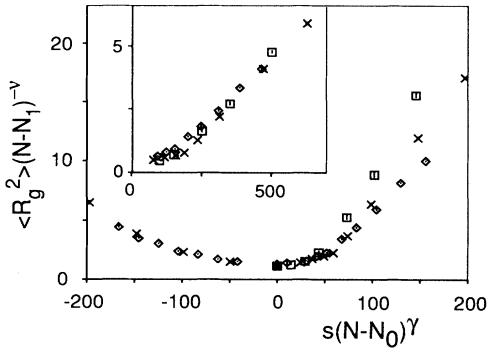

FIG. 2. Scaled radius of gyration, $\langle R_g^2\rangle(N-N_1)^{-\nu}$, as a function of the scaled flow rate $s(N-N_0)^\gamma$, with $\nu = \nu_{\rm bp} = 1$, $\gamma = 2$, $N_0 = 25$, and $N_1 = 30$. Data are shown for $N = 127$ ($\diamond$), $N = 247$ ($\times$), and $N = 407$ ($\square$). The inset shows the linear-polymer scaling behavior $\langle R_g^2\rangle(N-N_1)^{-\nu}$, as a function of $s(N-N_0)^\gamma$, with $\nu = 2\nu_{\rm lin} = 1.2$, $\gamma = 1 + 2\nu_{\rm lin} = 2.2$, $N_0 = 17$, and $N_1 = 32$.

that there is a crossover to *linear*-polymer behavior. In this case, the scaling form would again be given by (12), but with $\nu = 2\nu_{\rm lin} \simeq 6/5$ and $\gamma = 1 + 2\nu_{\rm lin} \simeq 11/5$. In fact, the data do appear to scale in this way for large s (see the inset in Fig. 2). Typical configurations for two different flow rates are shown in Fig. 3.

To understand the scaling form (12), we have to calculate the longest relaxation time of a self-avoiding branched polymer. This can be done as follows. At large length scales, a self-avoiding polymeric fractal can be described by an effective Gaussian Hamiltonian [29]

$$\mathcal{H}[\mathbf{R}] = \sum_{\mathbf{q}} q^\alpha \mathbf{R}_\mathbf{q}\mathbf{R}_{-\mathbf{q}}. \tag{13}$$

There are N different $\mathbf{q}$ vectors. Introducing the spectral dimension d_s, we can replace the sum over wave vectors by an integral,

$$\sum_{\mathbf{q}}(\,) \to N\int d^{d_s}q(\,). \tag{14}$$

This implies that the level spacing must be $\Delta q \sim N^{-1/d_s}$. To determine the exponent α in (13), we calculate the radius of gyration,

$$\langle R_g^2\rangle = \int_{q_{\rm min}} dq\; q^{d_s-1}\frac{1}{q^\alpha} \sim q_{\rm min}^{d_s-\alpha}. \tag{15}$$

With $q_{\rm min} \sim \Delta q$ and $\langle R_g^2\rangle^{d_f/2} \sim N$, where d_f is the fractal dimension, one arrives at [29]

$$\alpha = d_s(1 + 2/d_f). \tag{16}$$

The relaxation time is then obtained from the generalized Rouse equation,

$$\frac{\partial}{\partial t}\mathbf{R}_\mathbf{q} = \frac{\delta\mathcal{H}}{\delta\mathbf{R}}, \tag{17}$$

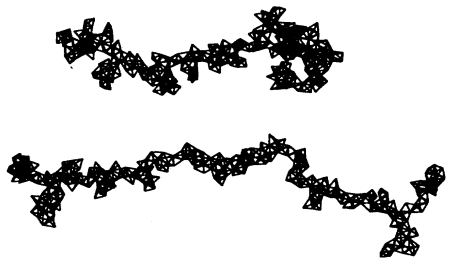

FIG. 3. Typical configurations of a vesicle with $N = 407$ monomers in elongational flow. The flow rates are $s = 0.0003$ (top) and $s = 0.0005$ (bottom).

which gives

$$\tau \sim q_{\rm min}^{-\alpha} \sim N^{1+2/d_f}. \tag{18}$$

Finally, we identify $2/d_f = \nu_{\rm bp} = 1$, which gives the scaling form (12).

We want to emphasize that in the derivation of (18) we have implicitly assumed that the connectivity of the network does not change, i.e., that the network remains a branched polymer at these flow rates. The problem can also be approached from the opposite point of view that the connectivity adjusts to the flow. In this case, the blob argument [11,30] for linear polymers under traction can be generalized to the present situation. Since the flow field is inhomogeneous, a position-dependent blob radius has to be used. This leads to the scaling behavior (18). It also predicts that the polymer should be more strongly stretched in the center of the chain [16], in agreement with the configurations shown in Fig. 3. It is reassuring to see that from the two arguments the same scaling behavior (18) emerges.

Finally, we want to investigate the possibility of a coil-stretched transition with increasing flow rate. In Fig. 4, we show a scaling plot of the fluctuations of the radius of gyration as a function of the scaled flow rate. For small

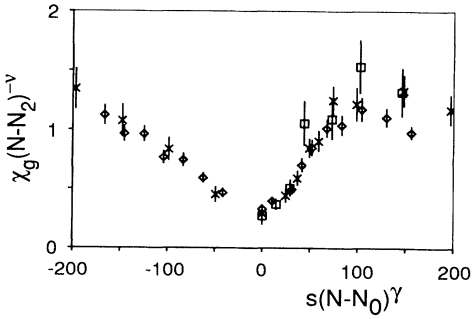

FIG. 4. Scaled fluctuations of the radius of gyration, $(N-N_2)^{-\nu_{\rm bp}}\chi_g$, as a function of the scaled flow rate $s(N-N_0)^\gamma$, with $\nu_{\rm bp} = 1$, $\gamma = 2$, $N_0 = 25$, and $N_2 = 40$. Data are shown for $N = 127$ ($\diamond$), $N = 247$ ($\times$), and $N = 407$ ($\square$).

flow rates, the data are consistent with the scaling form $\chi_g = N^{\nu_{bp}}\Xi(sN^{\gamma})$. The fluctuations have a maximum at $s(N - N_0)^{\gamma} \simeq 100$, which is approximately where the strongest increase of the radius of gyration is observed. However, the peak height increases only very weakly with increasing system size. A fit to the data gives $\chi_g \sim N^{\beta}$, with $\beta = 1.45 \pm 0.15$. For a first-order transition between a coiled state, with $\langle R_g^2 \rangle \sim N^{\nu}$, and a stretched state, with $\langle R_g^2 \rangle \sim N^2$, the radius distribution function, $P(R^2)$, has two sharp peaks centered at the average values of R_g^2 in the two phases. In the limit of large system size, where the peaks are well separated, the radius distribution can be approximated by

$$P(R^2) = \frac{1}{2}\left[\delta(R^2 - c_1 N^{\nu}) + \delta(R^2 - c_2 N^2)\right] , \quad (19)$$

with two constants c_1 and c_2. The susceptibility (11) is then easily calculated, and increases with an exponent $\beta = 2$ in this case. Thus, a first-order transition can be safely excluded.

In this paper, we have studied the behavior of highly flexible flaccid fluid vesicles in elongational flow. To understand the shape of erythrocytes, several other contributions, such as the bending energy, the shear elasticity [31], and volume constraints, as well as other types of flow geometries certainly have to be taken into account. This work is intended as a first step in that direction, and we hope that it will stimulate experiments on vesicles in elongational flow geometries.

We thank E. Evans for an inspiring conversation about the dynamical origin of the shape of erythrocytes. This work was supported in part by the University of Minnesota Army High Performance Computing Research Center, U.S. Army Contract No. DAAL03-89-C-0038, NATO Grant No. CRG910156, and the Deutsche Forschungsgemeinschaft through Sonderforschungsbereich 266.

[1] *Statistical Mechanics of Membranes and Surfaces*, edited by D.R. Nelson, T. Piran, and S. Weinberg (World Scientific, Singapore, 1989).
[2] R. Lipowsky, Nature (London) **349**, 475 (1991).
[3] W. Helfrich, Z. Naturforsch. **28c**, 693 (1973); H.J. Deuling and W. Helfrich, J. Phys. (Paris) **37**, 1335 (1976).
[4] P.G. de Gennes and C. Taupin, J. Chem. Phys. **86**, 2294 (1982).
[5] See, e.g., K. Berndl, J. Käs, R. Lipowsky, E. Sackmann, and U. Seifert, Europhys. Lett. **13**, 659 (1990), and references therein.
[6] H.P. Duwe, J. Käs, and E. Sackmann, J. Phys. (Paris) **51**, 945 (1990).
[7] D.M. Kroll and G. Gompper, in *Statistical Thermodynamics and Differential Geometry of Microstructured Materials*, edited by H.T. Davis and J.C.C. Nitsche (Springer, New York, 1993).
[8] M. Wortis, U. Seifert, K. Berndl, B. Fourcade, L. Miao, M. Rao, and R.K.P. Zia, in *Dynamical Phenomena at Interfaces, Surfaces and Membranes*, edited by D. Beysens, N. Boccara, and G. Forgacs (Nova Science, Commack, NY, 1991).
[9] A. Elgsaeter, B. Stokke, A. Mikkelsen, and D. Branton, Science **234**, 1217 (1986).
[10] B. Alberts, D. Bray, J. Lewis, R. Raff, K. Roberts, and J.D. Watson, *Molecular Biology of the Cell* (Garland, New York, 1983).
[11] P.-G. de Gennes, *Scaling Concepts in Polymer Physics* (Cornell University Press, Ithaca, NY, 1979).
[12] In experiments a two-dimensional flow field is often used; see, e.g., J.A. Odell, A. Keller, and Y. Rabin, J. Chem. Phys. **88**, 4022 (1988).
[13] G.G. Al-Noaimi, G.C. Martinez-Meller, and C.A. Wilson, J. Phys. (Paris), Lett. **39**, 373 (1978); K. Yamazaki and T. Ohta, J. Phys. A **15**, 287 (1982).
[14] P.-G. de Gennes, J. Chem. Phys. **60**, 5030 (1974).
[15] J.A. Odell and A. Keller, J. Polym. Sci. Polym. Phys. Ed. **24**, 1889 (1986).
[16] F.S. Henyey and Y. Rabin, J. Chem. Phys. **82**, 4362 (1985).
[17] J.J. Lopez Cascales and J. Garcia de la Torre, J. Chem. Phys. **95**, 9384 (1991).
[18] A. Billoire and F. David, Nucl. Phys. **B275**, 617 (1986); D.V. Boulatov, V.A. Kazakov, I.K. Kostov, and A.A. Migdal, Nucl. Phys. **B275**, 641 (1986).
[19] J.-S. Ho and A. Baumgärtner, Europhys. Lett. **12**, 295 (1990); A. Baumgärtner and J.-S. Ho, Phys. Rev. A **41**, 5747 (1990).
[20] D.M. Kroll and G. Gompper, Science **255**, 968 (1992).
[21] D. Boal and M. Rao, Phys. Rev. A **45**, R6947 (1992).
[22] D.M. Kroll and G. Gompper, Phys. Rev. A **46**, 3119 (1992).
[23] J.A. Aronovitz and D.R. Nelson, J. Phys. (Paris) **47**, 1445 (1986); J.A. Aronovitz and M.J. Stephen, J. Phys. A **20**, 2539 (1987).
[24] G. Gompper and D.M. Kroll, Europhys. Lett. **19**, 581 (1992); Phys. Rev. A **46**, 7466 (1992).
[25] G. Parisi and N. Sourlas, Phys. Rev. Lett. **46**, 871 (1981).
[26] Note that the exponent ν of the radius of gyration is defined differently for polymers, where $\sqrt{\langle R_g^2 \rangle} \sim N^{\nu}$, and for vesicles, where $\langle R_g^2 \rangle \sim N^{\nu}$. Therefore, $\nu_{bp} = 1$ is the vesicle exponent in the branched-polymer regime.
[27] It can be shown exactly that the derivative of $\langle R_g^2 \rangle$ and Δ_3 (as well as of other quantities) with respect to s vanishes identically at $s = 0$. Thus, all scaling functions must have an extremum at $s = 0$.
[28] C.J. Camacho and M.E. Fisher, Phys. Rev. Lett. **65**, 9 (1990).
[29] M.E. Cates, Phys. Rev. Lett. **53**, 926 (1984); J. Phys. (Paris) **46**, 1059 (1985).
[30] P. Pincus, Macromolecules **9**, 386 (1976).
[31] The simple tether-and-bead model for fluid membranes considered here has been extended as a model for the erythrocyte membrane by D. Boal, U. Seifert, and A. Zilker, Phys. Rev. Lett. **69**, 3405 (1992).